

Identification of *katG* Mutations Associated with High-Level Isoniazid Resistance in *Mycobacterium tuberculosis*^{∇†}

Hiroki Ando,¹ Yuji Kondo,² Toshinori Suetake,² Emiko Toyota,³
Seiya Kato,⁴ Toru Mori,⁴ and Teruo Kirikae^{1*}

Department of Infectious Diseases, Research Institute, International Medical Center of Japan, 1-21-1 Toyama, Shinjuku, Tokyo 162-8655, Japan¹; Third Department, Research and Development Laboratory, Nipro Corporation, 3023 Noji, Kusatsu, Shiga 525-0055, Japan²; National Hospital Organization Tokyo National Hospital, 3-1-1 Takeoka, Kiyose, Tokyo 204-8585, Japan³; and Research Institute of Tuberculosis, Japan Anti-Tuberculosis Association, 3-1-24 Matsuyama, Kiyose, Tokyo 204-8533, Japan⁴

Received 2 December 2009/Returned for modification 28 December 2009/Accepted 25 February 2010

Isoniazid (INH) is an effective first-line antituberculosis drug. KatG, a catalase-peroxidase, converts INH to an active form in *Mycobacterium tuberculosis*, and *katG* mutations are major causes of INH resistance. In the present study, we sequenced *katG* of 108 INH-resistant *M. tuberculosis* clinical isolates. Consequently, 9 novel KatG mutants with a single-amino-acid substitution were found. All of these mutants had significantly lower INH oxidase activities than the wild type, and each mutant showed various levels of activity. Isolates having mutations with relatively low activities showed high-level INH resistance. On the basis of our results and known mutations associated with INH resistance, we developed a new hybridization-based line probe assay for rapid detection of INH-resistant *M. tuberculosis* isolates.

Isoniazid (INH) is an effective drug used in the treatment of tuberculosis and has been in common use to treat tuberculosis since its introduction in 1952 (4). However, the emergence of INH-resistant (Inh^r) *Mycobacterium tuberculosis* is jeopardizing the continued utility of INH (10).

Drug resistance in *M. tuberculosis* is caused by mutations in restricted regions of the genome (36). Mutations in *katG*, the upstream region of the *fabG1-inhA* operon (P_{*fabG1-inhA*}), and *inhA* are responsible for INH resistance (36). The *katG* gene encodes the bifunctional catalase-peroxidase enzyme that converts INH to an active form (35).

Previously, we developed a DNA sequencing-based method to detect mutations in regions associated with INH resistance in *M. tuberculosis*, including *katG* and P_{*fabG1-inhA*} (28). Consequently, five novel mutations in *katG* associated with INH resistance were found (28). In the present study, we cloned 21 *katG* mutants, including 15 novel mutants, and compared their INH oxidase activities. Certain *katG* mutations were shown to cause high-level INH resistance, which suggests the possibility of determining the degree of INH resistance, such as high- or low-level resistance, by detecting these *katG* mutations. Furthermore, to detect these mutations in ordinary-scale clinical laboratories without sequencing, we developed a new hybridization-based line probe assay (LiPA) for INH resistance in *M. tuberculosis* isolates, which can be applied easily in clinical use.

* Corresponding author. Mailing address: Department of Infectious Diseases, Research Institute, International Medical Center of Japan, 1-21-1 Toyama, Shinjuku, Tokyo 162-8655, Japan. Phone: (81)-3-3202-7181, ext. 2838. Fax: (81)-3-3202-7364. E-mail: tkirikae@ri.imcj.go.jp.

† Supplemental material for this article may be found at <http://aac.asm.org/>.

[∇] Published ahead of print on 8 March 2010.

MATERIALS AND METHODS

Bacterial strains and plasmids. One hundred eight Inh^r *M. tuberculosis* isolates were obtained from single patients at the International Medical Center of Japan and National Hospital Organization Tokyo National Hospital from 2003 to 2008. INH-susceptible (Inh^s) *M. tuberculosis* strains H37Rv and IMCJ 2751 were used. The IMCJ 2751 isolate has a *katG*(G1388T) [KatG(R463L)] neutral mutation. The *Escherichia coli* strains and plasmids used in this study are listed in Table 1. *E. coli* TOP10F' (Invitrogen, Carlsbad, CA) was used as the host for cloning. *E. coli* UM262 (17) was used as the host for expression of *katG* derived from clinical isolates and H37Rv.

Drug susceptibility testing. All clinical isolates, H37Rv, and IMCJ 2751 were tested for drug susceptibility. Strains were analyzed by an agar proportion method with egg-based Ogawa medium (Vit Spectrum-SR [Kyokuto Pharmaceutical Industrial Co., Tokyo, Japan] or Wellpack [Japan BCG Laboratory, Tokyo, Japan]), which is based on a slightly modified WHO protocol (3) and is recommended by the Japanese Society of Tuberculosis (3, 12). The medium contained INH (0.2 µg/ml and 1.0 µg/ml), rifampin (RIF) (40 µg/ml), ethambutol (EB) (2.5 µg/ml), kanamycin (KM) (20 µg/ml), *p*-aminosalicylic acid (PAS) (0.5 µg/ml), streptomycin (SM) (10 µg/ml), ethionamide (TH) (20 µg/ml), enviomycin (EVM) (20 µg/ml), cycloserine (CS) (30 µg/ml), and levofloxacin (LVFX) (1.0 µg/ml). The results of drug susceptibility testing are shown in Table S1 in the supplemental material.

Isolation of genomic DNA. Genomic DNA from *M. tuberculosis* was extracted as described previously (22).

DNA sequencing of INH resistance-related genes. The *furA-katG* operon and its upstream region were amplified by PCR with primers -129*furA* (5'-GCTCA TCGGAACATACGAAG-3') and *katG*+50 (5'-GTGCTGCGGCGGTTGTG GTTGATCGGCGG-3'). The *fabG1-inhA* operon and P_{*fabG1-inhA*} were also amplified, using primers -200*fabG1* (5'-TTCGTAGGGCGTCAATACAC-3') and *inhA*+40 (5'-CCGAACGACAGCAGCAGGAC-3'). PCR products were used as templates for direct DNA sequencing. DNA sequences were compared with the H37Rv sequence using Genetyx-Mac, version 14.0.2 (Genetyx Corporation, Tokyo, Japan).

Construction of plasmids. The coding regions of *katG* from H37Rv, IMCJ 2751, and Inh^r clinical isolates with *katG* mutations were amplified by PCR with the primers *katG*-F-ccc (5'-CCCGAGCAACACCCACCCATTACAGAAAC-3') and *katG*-R (5'-TCAGCGCACGTGCGAACC-3') and cloned into pTrcHis2-TOPO (Invitrogen) using the TA cloning method. The pTrcHis2-TOPO vector encodes a C-terminal peptide containing a c-myc epitope and a 6×His tag. However, the expressed recombinant KatG protein did not have any additional amino acid residues, such as the c-myc epitope and the 6×His tag, because the

TABLE 1. *E. coli* strains and plasmids used in this study

Strain or plasmid	Genotype or description	Source or reference
<i>E. coli</i> strains		
TOP10F'	F' [<i>lacI</i> ^q Tn10 (Tet ^r)] <i>mcrA</i> Δ (<i>mrr-hsdRMS-mcrBC</i>) ϕ 80 <i>lacZ</i> Δ M15 Δ <i>lacX74</i> <i>recA1 araD139</i> Δ (<i>ara-leu</i>)7697 <i>galU galK rpsL</i> (Str ^r) <i>endA1 nupG</i>	Invitrogen
UM262	<i>katG::Tn10 recA pro leu rpsL hsdM hsdR endl lacY</i>	17
Plasmids		
pTrcHis2-TOPO	TA cloning and expression vector; Ap ^r Km ^r	Invitrogen
<i>pkatG</i> -wt	pTrcHis2-TOPO carrying <i>katG</i>	This study
<i>pkatG</i> -1	<i>pkatG</i> -wt carrying G1388T (neutral mutation)	This study
<i>pkatG</i> -2	<i>pkatG</i> -1 carrying C379G	This study
<i>pkatG</i> -3	<i>pkatG</i> -1 carrying C694T	This study
<i>pkatG</i> -4	<i>pkatG</i> -wt carrying A398C	This study
<i>pkatG</i> -5	<i>pkatG</i> -1 carrying T1147C	This study
<i>pkatG</i> -6	<i>pkatG</i> -1 carrying 1297::C, Δ 1305C	This study
<i>pkatG</i> -7	<i>pkatG</i> -1 carrying a290g	This study
<i>pkatG</i> -8	<i>pkatG</i> -1 carrying C1465A	This study
<i>pkatG</i> -9	<i>pkatG</i> -wt carrying G944C	This study
<i>pkatG</i> -10	<i>pkatG</i> -1 carrying T1259C	This study
<i>pkatG</i> -11	<i>pkatG</i> -wt carrying G944C, G1159C	This study
<i>pkatG</i> -12	<i>pkatG</i> -1 carrying G368A, G895A	This study
<i>pkatG</i> -13	<i>pkatG</i> -1 carrying G1255C	This study
<i>pkatG</i> -14	<i>pkatG</i> -1 carrying C195T (silent mutation), T527C	This study
<i>pkatG</i> -15	<i>pkatG</i> -wt carrying Δ (478–479)	This study
<i>pkatG</i> -16	<i>pkatG</i> -1 carrying G944C	This study
<i>pkatG</i> -17	<i>pkatG</i> -wt carrying Δ 371G	This study
<i>pkatG</i> -18	<i>pkatG</i> -1 carrying C1894T	This study
<i>pkatG</i> -19	<i>pkatG</i> -wt carrying C945A	This study
<i>pkatG</i> -20	<i>pkatG</i> -1 carrying Δ (571–576)	This study
<i>pkatG</i> -21	<i>pkatG</i> -1 carrying G1624C	This study

katG-R reverse primer included the native stop codon. The DNA sequences of all clones were confirmed by sequencing.

RFLP. IS6110-probed restriction fragment length polymorphism (RFLP) was performed as described previously (22). Patterns with more than 70% similarity were postulated to form a cluster.

Immunoblotting. Proteins separated by SDS-PAGE were transferred onto Immobilon-Blot polyvinylidene difluoride (PVDF) membranes (Bio-Rad, Hercules, CA). The proteins on the membranes were detected using primary antibodies specific for KatG (28). KatG was visualized with horseradish peroxidase-conjugated secondary antibodies.

Enzyme assays. KatG mediates free-radical formation from INH oxidation in the presence of H₂O₂. The activities of KatG were detected spectrophotometrically by following the reduction of nitroblue tetrazolium (NBT) at A₅₆₀ (28, 32). Peroxidase activity was monitored spectrophotometrically by following the oxidation of 2,2'-azino-bis(3-ethylbenzothiazoline-6-sulfonic acid) (ABTS) at A₄₀₅ (21). Catalase activity was measured spectrophotometrically by following the degradation of H₂O₂ at A₂₄₀ (21). The catalase activity is shown as values subtracted from that of the vector control. All assays were carried out at 25°C. The absorbance was read 200 s after the initiation of the reaction.

LiPA. The line probe assay (LiPA) was performed as described previously (1, 29). In brief, 41 oligonucleotide probes were designed to cover mutations in the *furA-katG* (35 probes for *katG* and 2 for *furA*), *P_{fabG1-inhA}* (2 probes), and *fabG1* (2 probes) regions (Table 2). These probes were immobilized on two strips. Six regions, located within *P_{fabG1-inhA}* (477 bp), *fabG1* (209 bp), *furA* (256 bp), and *katG* (612 bp, 698 bp, and 907 bp), were amplified by nested PCR. Immobilized probes on the two strips were hybridized with the biotinylated PCR products and then incubated with streptavidin labeled with alkaline phosphatase. The color development was performed by incubation with 5-bromo-4-chloro-3'-indolylphosphatase *p*-toluidine and NBT.

RESULTS

Drug susceptibility profiles. As shown in Table S1 in the supplemental material, among 108 Inh^r isolates, 65 (60%) were resistant to INH at 0.2 μ g/ml but susceptible to INH at 1.0

μ g/ml. The remaining 43 (40%) were resistant to INH at 1.0 μ g/ml. Among the 108 isolates, 44 (41%) were resistant to INH but susceptible to other antituberculosis drugs. Thirteen (12%) were multidrug-resistant (MDR) isolates and five (5%) were extensively drug resistant (XDR).

IS6110-probed RFLP. The results of IS6110-probed fingerprinting of the 108 Inh^r isolates are shown in Fig. S1 in the supplemental material. Five clusters were detected, consisting of a total of 63 isolates (58%), including 12 (11%) in cluster I, 22 (20%) in cluster II, 12 (11%) in cluster III, 12 (11%) in cluster IV, and 5 (5%) in cluster V. These observations suggested that the majority of Inh^r isolates in Japan expanded in a clonal manner.

Correlation between drug susceptibility and IS6110-probed RFLP. With regard to the degree of INH resistance, the proportions of high-level Inh^r isolates, i.e., isolates resistant to INH (1.0 μ g/ml), were 1 (8%) in cluster I, 8 (36%) in cluster II, 4 (33%) in cluster III, 4 (33%) in cluster IV, and 5 (100%) in cluster V. These results indicated that the majority of isolates belonging to cluster I were resistant to INH (0.2 μ g/ml) and susceptible to INH (1.0 μ g/ml) and that those belonging to cluster V were highly resistant to INH. Six of 13 MDR isolates (46%) and 1 of 5 XDR isolates (20%) belonged to the clusters, but other MDR and XDR isolates did not belong to any clusters, indicating that they emerged sporadically in Japan.

Mutations in *furA-katG*, *fabG1-inhA*, and their upstream regions. We sequenced the *furA-katG* operon, the *fabG1-inhA* operon, and their upstream regions in all Inh^r isolates tested. Of the 108 isolates, 105 had at least one mutation (see Table S1

TABLE 2. Locations of 41 oligonucleotide probes designed to cover a mutation(s) associated with INH resistance

Probe	Amino acid (nucleotide) region covered by probe
<i>inhA</i> -1.....	(-17 to -3) ^a
<i>inhA</i> -2.....	95-100
<i>fabG1</i> -1.....	202-206
<i>fabG1</i> -2.....	230-235
<i>furA</i> -1.....	12-17
<i>furA</i> -2.....	6-12
<i>katG</i> -1.....	45-51
<i>katG</i> -2.....	63-68
<i>katG</i> -3.....	92-97
<i>katG</i> -4.....	94-99
<i>katG</i> -5.....	105-111
<i>katG</i> -6.....	123-127
<i>katG</i> -7.....	132-137
<i>katG</i> -8.....	135-140
<i>katG</i> -9.....	140-145
<i>katG</i> -10.....	157-163
<i>katG</i> -11.....	170-174
<i>katG</i> -12.....	174-179
<i>katG</i> -13.....	178-183
<i>katG</i> -14.....	190-194
<i>katG</i> -15.....	228-236
<i>katG</i> -16.....	247-252
<i>katG</i> -17.....	256-261
<i>katG</i> -18.....	271-277
<i>katG</i> -19.....	294-299
<i>katG</i> -20.....	313-318
<i>katG</i> -21.....	323-327
<i>katG</i> -22.....	326-330
<i>katG</i> -23.....	383-387
<i>katG</i> -24.....	389-391
<i>katG</i> -25.....	417-422
<i>katG</i> -26.....	457-462
<i>katG</i> -27.....	479-482
<i>katG</i> -28.....	486-490
<i>katG</i> -29.....	522-528
<i>katG</i> -30.....	539-543
<i>katG</i> -31.....	553-558
<i>katG</i> -32.....	565-569
<i>katG</i> -33.....	591-596
<i>katG</i> -34.....	631-635
<i>katG</i> -35.....	707-712

^a Nucleotide position relative to the initiation codon of *fabG1*.

in the supplemental material), while the remaining 3 had no mutations in the regions sequenced. Of the 105 isolates with mutations, 64 had mutations in the *furA-katG* operon, 62 had mutations in *fabG1-inhA* operon, and 21 had mutations in both regions. Of the 64 with mutations in the *furA-katG* operon, six had a large-scale deletion adjacent to the *furA-katG* operon (Fig. 1; see also Table S1 in the supplemental material). As shown by genetic maps (Fig. 1), these isolates had large-scale deletions, ranging in size from 2.3 to 34.4 kb. The remaining 58 isolates did not have large-scale deletions.

Twenty-eight different mutations were found among the 58 isolates with mutations in the *furA-katG* operon (see Table S1 in the supplemental material). Twenty-three were in *katG*, two were in *furA*, and three were in the intergenic region. Seven different mutations were found among the 62 isolates with mutations in the *fabG1-inhA* operon (see Table S1 in the supplemental material). Three were in the upstream region, two were in *fabG1*, and two were in *inhA*. Of the 28 different mutations found in the *furA-katG* operon, 22 were novel (2 in

furA, 3 in the intergenic region of the *furA-katG* operon, and 17 in *katG*). Of the seven different mutations found in the *fabG1-inhA* operon, four were novel: one in the upstream region of the *fabG1-inhA* operon, two in *fabG1*, and one in *inhA* (see Table S1 in the supplemental material).

Correlation between INH resistance and mutations. We recently reported 5 novel mutations in *katG* (28). Including these mutations, 280 different mutations in *katG* were found in PubMed (<http://www.ncbi.nlm.nih.gov/sites/entrez?db=pubmed>) when articles were searched by the keywords “*katG*,” “mutation,” and “tuberculosis.” In addition, six mutations in the upstream region of the *fabG1-inhA* operon, including C-15T, and seven in *inhA* cause INH resistance (27, 28, 36). In this study, we found an additional 17 novel mutations in *katG*. One was a silent mutation (C195T [A65A]), while the other 16 caused amino acid substitutions. These mutations and amino acid substitutions are shown in Table 3. Furthermore, several novel mutations were detected in the present study: one in *fabG1* (G609A [L203L]), one in *furA* (C41T [A14V]), and three in the intergenic region of the *furA-katG* operon (G-7A, A-10C, and G-12A).

We will report elsewhere that these mutations in *furA* and the intergenic region are associated with INH resistance induced by downregulation of *katG* expression (H. Ando and T. Kirikae, unpublished results), and those in *fabG1* are also associated with INH resistance induced by upregulation of *inhA* expression (Ando et al., unpublished). In the present study, we examined whether novel mutations in *katG* are associated with INH resistance.

Correlation between mutations and IS6110-probed RFLP. As shown in Fig. S1 and Table S1 in the supplemental material, all isolates belonging to cluster I detected in the IS6110-probed RFLP analysis, 11 (50%) in cluster II, and 8 (67%) in cluster III had a C-15T mutation in the *inhA* promoter region. All isolates in cluster IV had a C41T mutation in *furA*. All isolates in cluster V had a G944C/G945A (S315T/R) mutation. Isolates harboring *katG* mutations, except those with the G944C/G945A (S315T/R) mutation, did not cluster in the IS6110-probed RFLP.

Enzymatic activity of the novel KatG mutants. We cloned a wild-type (WT) *katG* gene (*pkatG*-wt) from H37Rv, a *katG* gene carrying a G1388T neutral mutation (*pkatG*-1) from IMCJ 2751, and 20 *katG* genes harboring mutations causing amino acid substitutions (*pkatG*-2 to -21) from *Inh*^r isolates (Tables 1 and 3). Among the mutants, 15 were novel and 6 had been reported previously (the *katG*-1, -7, -9, -13, -16, and -19 mutants) (Table 3). These *katG* genes were expressed in *katG*-deficient *E. coli* UM262. As shown in Fig. 2, *E. coli* isolates with *katG*-wt expressed KatG (lanes 1 and 15), whereas *E. coli* isolates with an empty vector did not (lanes 2 and 16). *E. coli* isolates carrying *katG* mutants other than the *katG*-15 (lane 8) and *katG*-17 (lane 24) mutants expressed KatG proteins at levels similar to those observed for *E. coli* isolates carrying *pkatG*-wt. *E. coli* isolates with *katG*-15 (lane 8) and *katG*-17 (lane 24), which had a frame shift mutation (Table 3), did not express *katG*.

INH oxidase, peroxidase, and catalase activities were assessed using these clones (Table 4). Of the cloned mutants, one with KatG(R463L) from IMCJ 2751 showed levels of these activities similar to those observed for the wild type, and the KatG(R463L) mutation was not associated with INH resis-

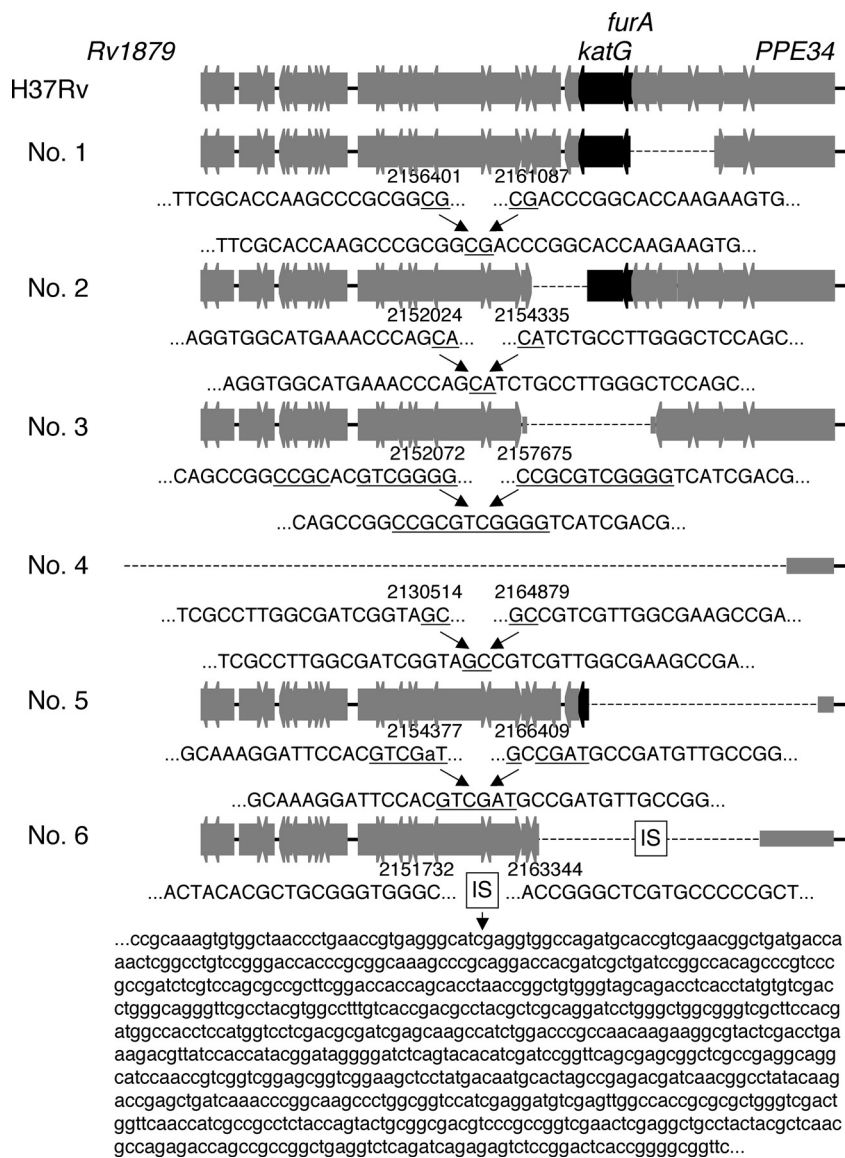


FIG. 1. Maps of large-scale deleted regions adjacent to *katG* in six InH⁺ *M. tuberculosis* isolates. Bold arrows indicate the open reading frames annotated in the H37Rv genome sequence (<http://genolist.pasteur.fr/TubercuList/>). The dotted lines correspond to the deleted regions, with the end sequences and H37Rv genome coordinates given below. Underlined sequences are possible substrates for recombination. The box labeled "IS" represents the 750-bp fragment of IS6110. Numbers 1 to 6 represent the names of the isolates and correspond to the numbers shown in Table S1 in the supplemental material. A nucleotide shown in lowercase in region 5 indicates a mutation.

tance (Table 4). With regard to INH oxidase activity, *E. coli* isolates with *katG*-2 to -8 showed 1/3 to 1/17 less activity than those with *katG*-wt. *E. coli* isolates carrying *katG*-9 to -13 showed reduced activity compared to those carrying *katG*-2 to -8. *E. coli* isolates carrying *katG*-14 to -21 showed no activity (i.e., levels similar to those observed for vector controls). These results indicated that the degree of INH oxidase activity is correlated with that of INH resistance. *E. coli* isolates with *katG*-wt and *katG*-1 showed the highest levels of INH oxidase activity, and *M. tuberculosis* isolates with these genes were sensitive to INH. *E. coli* isolates carrying *katG*-2 to -8 showed slightly weaker activities, and *M. tuberculosis* isolates with these genes were resistant to INH at 0.2 $\mu\text{g/ml}$ but susceptible to INH at 1.0 $\mu\text{g/ml}$. *E. coli* isolates with *katG*-9 to -21 showed

weak or no activity, and *M. tuberculosis* isolates with these genes were resistant to INH at 1.0 $\mu\text{g/ml}$.

The peroxidase and catalase activities of *E. coli* isolates with mutations were correlated well with each other and also with INH oxidase activity (Table 4). However, in *E. coli* isolates carrying some clones, peroxidase/catalase activities were different from INH oxidase activity, i.e., *E. coli* isolates with *katG*-16 and -9 showed weak activity.

Development of a LiPA for detection of INH resistance. To detect novel mutations associated with INH resistance, we developed a new LiPA based on the reverse hybridization principle (25). Forty-one oligonucleotide probes were designed for the LiPA to detect mutations containing the *furA*-*katG* operon, the *fabG1*-*inhA* operon, P_{*fabG1*-*inhA*}, and *fabG1* (Table

TABLE 3. *katG* mutations found in *Inh^r* isolates

Clone	Mutation(s)	
	Nucleotide	Amino acid
<i>katG</i> -1 ^a	G1388T	R463L
<i>katG</i> -2 ^c	C379G ^b	Q127E ^b
<i>katG</i> -3 ^c	C694T ^b	P232S ^b
<i>katG</i> -4	A398C ^b	N133T ^b
<i>katG</i> -5 ^c	T1147C ^b	S383P ^b
<i>katG</i> -6 ^c	1297::C ^b , Δ1305C ^b	KQT433-435QAD ^b
<i>katG</i> -7 ^c	A290G	H97R
<i>katG</i> -8 ^c	C1465A ^b	R489S ^b
<i>katG</i> -9	G944C	S315T
<i>katG</i> -10 ^c	T1259C ^b	M420T ^b
<i>katG</i> -11	G944C, G1159C ^b	S315T, D387H ^b
<i>katG</i> -12 ^c	G368A ^b , G895A	G123E ^b , G299S
<i>katG</i> -13 ^c	G1255C	D419H
<i>katG</i> -14 ^c	C195T ^b , T527C ^b	A65A ^b , M176T ^b
<i>katG</i> -15	Δ(478–479) ^b	Frame shift ^b
<i>katG</i> -16 ^c	G944C	S315T
<i>katG</i> -17	Δ371G ^b	Frame shift ^b
<i>katG</i> -18 ^c	C1894T ^b	R632C ^b
<i>katG</i> -19	C945A	S315R
<i>katG</i> -20 ^c	Δ(571–576) ^b	Δ(191W-192E) ^b
<i>katG</i> -21 ^c	G1624C ^b	D542H ^b

^a *katG*-1 carrying a G1388T (R463L) neutral mutation was cloned from the *Inh^s* strain IMCJ 2751.

^b These mutations have not previously been reported. Other mutations were previously reported in references 36 (G1388T), 7 (A290G), 36 (G944C), 7 (G895A), 6 (G1255C), and 36 (C945A).

^c This clone also had a G1388T neutral mutation.

2). As shown in Fig. S2 in the supplemental material, the LiPA could detect all mutations found in this study.

DISCUSSION

The results of RFLP and sequence analysis in the present study indicated that there are several predominant strains of *Inh^r* *M. tuberculosis* with different genetic backgrounds in Japan (see Fig. S1 and Table S1 in the supplemental material). These strains had *katG*(G944C) (S315T), an *inhA* promoter mutation, *fabG1*(G609A) (L203L), and *furA*(C41T) (A14V) (see Table S1 in the supplemental material). *Inh^r*

isolates were reported to expand clonally in several regions, including northwestern Russia (20), the Netherlands (30), San Francisco, CA (13), Venezuela (2), and Sierra Leone (15). These clonal *Inh^r* strains had a *KatG*(S315T) or *inhA* promoter mutation. Gagneux et al. (13) reported that the strains carrying the *KatG*(S315T) or *inhA* promoter mutation were more likely to spread than those carrying other mutations; our results were consistent with these previous findings. In addition, strains with *fabG1*(G609A) (L203L) and *furA*(C41T) (A14V) mutations were also more likely to spread in Japan.

Of *Inh^r* isolates, a smaller number (22%) had S315T/R mutations in Japan (Table S1). The prevalences of the *KatG*(S315T) mutation in *M. tuberculosis* strains from around the world differ, especially with regard to the prevalence of tuberculosis. In regions where the prevalence of tuberculosis is low or intermediate, the mutation has been reported relatively infrequently: it occurred in 26% to 30% of 95 isolates from Singapore (16) and Madrid (23) and rarely in isolates from Scotland (11) and Finland (19). In contrast, the S315T mutation accounted for INH resistance in 52% to 64% of strains in Africa (8, 14, 31), 79% in Peru (9), 91% in Russia (18), and 58% in New York, NY. (23).

We found four *KatG* mutations (D419H, M420T, D542H, and R632C) that are associated with high-level INH resistance, and we also found three *KatG* mutations (H97R, N133T, and P232S) that are associated with low-level INH resistance (Table 4). The S315 mutation is known to confer high-level INH resistance (24, 26, 33). *KatG* is a functional homodimer, and each monomer is composed of two domains that are mainly α -helical. The N-terminal domain contains a heme binding site, whereas the C-terminal domain lacks this feature (34). The high-level INH resistance-associated mutations D419H and M420T are located in the region connecting the N-terminal and C-terminal domains (5). The interdomain interactions between the N-terminal and C-terminal domains of the two monomers are essential for forming the functional homodimer (5). The changes in the interdomain interactions due to the D419H and M420T mutations may result in loss of enzymatic activities of *KatG*. D542H and R632C are located in the 16th

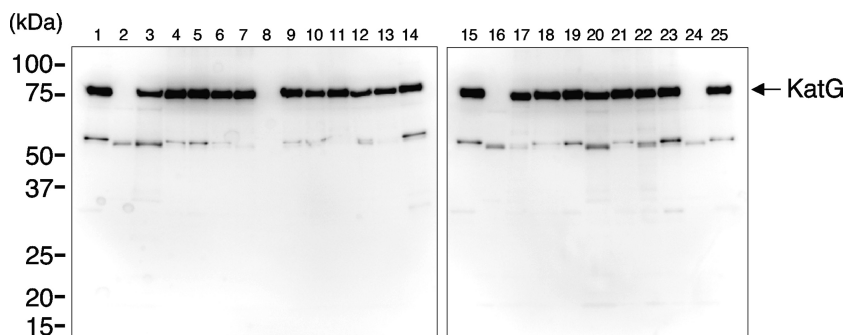


FIG. 2. Western blot of whole-cell extracts from *katG*-deficient *E. coli* strain UM262 transformed with the empty vector, pTrcHis2-TOPO, or recombinant plasmids expressing various *KatG* mutations as follows: lanes 1 and 15, WT; lanes 2 and 16, empty vector; lane 3, R463L and D542H; lane 4, S315T and R463L; lane 5, Q127E and R463L; lane 6, P232S and R463L; lane 7, G123E, G299S, and R463L; lane 8, frame shift mutation from position 160; lane 9, S315T and D387H; lane 10, R463L and R489S; lane 11, S315R; lane 12, M420T and R463L; lane 13, A65A, M176T, and R463L; lane 14, H97R and R463L; lane 17, Δ(191W-192E) and R463L; lane 18, N133T; lane 19, R463L; lane 20, R463L and R632C; lane 21, S315T; lane 22, D419H and R463L; lane 23, S383P and R463L; lane 24, frame shift mutation from position 124; lane 25, in-frame insertion and deletion and R463L. The positions of molecular mass markers are shown on the left.

TABLE 4. Enzymatic activities of KatG mutants detected in this study

Plasmid	Amino acid mutation(s)		Mean activity \pm SD ^a			Additional mutation associated with INH resistance	INH resistance level ^b
	Not previously reported	Previously reported	INH oxidase (10 ³ A ₅₆₀ units)	Peroxidase (10 ² A ₄₀₅ units)	Catalase (10 ² A ₂₄₀ units)		
pTrcHis2-TOPO ^c			4.84 \pm 0.17	6.89 \pm 0.70	0.00 \pm 0.24		
<i>pkatG</i> -wt			177.16 \pm 18.50	286.08 \pm 0.43	142.26 \pm 0.16		S
<i>pkatG</i> -1		R463L	162.00 \pm 11.31	289.62 \pm 1.40	141.85 \pm 0.13		S
<i>pkatG</i> -2	Q127E	R463L	60.18 \pm 0.95	256.07 \pm 7.80	143.21 \pm 0.35	P _{<i>fabG1-inhA</i>} C-15T	0.2
<i>pkatG</i> -3	P232S	R463L	54.47 \pm 0.36	62.25 \pm 0.05	76.63 \pm 0.52		0.2
<i>pkatG</i> -4	N133T		40.67 \pm 6.31	36.00 \pm 0.26	100.61 \pm 5.55		0.2
<i>pkatG</i> -5	S383P	R463L	38.49 \pm 0.04	42.24 \pm 3.64	107.65 \pm 4.13	P _{<i>fabG1-inhA</i>} C-15T	0.2
<i>pkatG</i> -6	KQT433-435QAD ^d	R463L	20.02 \pm 0.48	106.47 \pm 1.17	142.81 \pm 0.11	P _{<i>fabG1-inhA</i>} C-15T	0.2
<i>pkatG</i> -7		H97R, R463L	17.42 \pm 0.35	26.80 \pm 0.44	27.86 \pm 2.01		0.2
<i>pkatG</i> -8	R489S	R463L	10.40 \pm 0.16	27.34 \pm 0.27	14.83 \pm 0.93	P _{<i>fabG1-inhA</i>} C-15T	0.2
<i>pkatG</i> -9		S315T	8.83 \pm 0.04	102.00 \pm 2.54	71.26 \pm 1.71		1.0
<i>pkatG</i> -10	M420T	R463L	8.42 \pm 0.14	21.02 \pm 0.37	46.45 \pm 0.20		1.0
<i>pkatG</i> -11	D387H	S315T	7.93 \pm 0.08	34.75 \pm 0.61	35.71 \pm 0.41		1.0
<i>pkatG</i> -12	G123E	G299S, R463L	6.87 \pm 0.66	6.02 \pm 0.17	-0.70 \pm 1.42	P _{<i>fabG1-inhA</i>} T-8C	1.0
<i>pkatG</i> -13		D419H, R463L	6.30 \pm 0.52	7.67 \pm 0.01	4.49 \pm 0.39		1.0
<i>pkatG</i> -14	M176T ^e	R463L	5.14 \pm 0.01	4.67 \pm 0.07	1.06 \pm 0.30	P _{<i>fabG1-inhA</i>} C-15T	1.0
<i>pkatG</i> -15	Frame shift ^f		5.02 \pm 0.24	4.01 \pm 0.57	-1.75 \pm 1.16		1.0
<i>pkatG</i> -16		S315T, R463L	3.83 \pm 0.18	84.41 \pm 0.17	117.07 \pm 7.56		1.0
<i>pkatG</i> -17	Frame shift ^g		3.30 \pm 0.69	4.59 \pm 0.09	2.07 \pm 1.51		1.0
<i>pkatG</i> -18	R632C	R463L	3.26 \pm 0.13	1.56 \pm 0.08	-7.41 \pm 0.76		1.0
<i>pkatG</i> -19		S315R	3.19 \pm 0.76	3.24 \pm 0.02	-2.36 \pm 0.71		1.0
<i>pkatG</i> -20	Δ (191W-192E) ^h	R463L	2.78 \pm 0.09	2.09 \pm 0.04	2.61 \pm 1.86		1.0
<i>pkatG</i> -21	D542H	R463L	1.63 \pm 0.49	0.32 \pm 0.17	-7.00 \pm 0.69		1.0

^a Mean ($n = 3$) \pm SD.

^b The INH susceptibility levels for clinical isolates with *katG* mutations are shown, as follows: S, INH sensitive; 0.2, resistant to INH (0.2 μ g/ml) and susceptible to INH (1.0 μ g/ml); and 1.0, resistant to INH (1.0 μ g/ml).

^c A vector control.

^d 1297::C and Δ 1305C.

^e This isolate had an additional A65A silent mutation.

^f Δ (478-479).

^g Δ 371G.

^h Δ (571-576).

and 19th α -helices in the C-terminal domain, respectively, and showed no enzymatic activities, although the functional role of the C-terminal domain in KatG remains unclear (5, 34). The mutations associated with low-level INH resistance, H97R, N133T, and P232S, are located adjacent to the INH binding pocket (5). They may weakly affect the binding affinity of INH. The S315T mutation located at the INH binding pocket could block binding of INH without interfering with catalysis (5).

The new LiPA was able to distinguish high-level INH resistance (resistant to 1.0 μ g/ml) from low-level INH resistance (resistant to 0.2 μ g/ml and sensitive to 1.0 μ g/ml) in clinical isolates without sequencing. Thus, we were able to determine the degree of INH resistance using this LiPA. This assay would be useful in clinical application in combination with culture-based drug susceptibility tests. We have recently developed a LiPA to detect a *pncA* mutation(s) for rapid detection of pyrazinamide-resistant *M. tuberculosis* (29), which was shown to be readily usable in clinical applications (1). The whole procedure takes only 9 h, and the estimated cost per sample is \$35. The clinical trials for *in vitro* diagnosis are in progress (from April 2009 to March 2010) in Japan. The trials will reveal the specificity of the LiPA. It will be beneficial especially in developing countries where the laboratories are scarcely equipped because of the high cost of setting them up.

Assessment of INH oxidase activities of *M. tuberculosis* isolates may provide useful information about INH resistance. The INH oxidase activities of KatG mutants showed good

correlations with the degree of INH resistance (Table 4). Other enzymatic activities of KatG mutants, i.e., peroxidase and catalase activities, were also correlated with the degree of INH resistance (Table 4). However, the activities of the S315T mutant were not, i.e., this mutant showed catalase-peroxidase activities but no INH oxidase activity (Table 4). Other S315 mutants, such as the S315R (Table 4) and S315N (32) mutants, have lost all three kinds of enzymatic activity. Thus, the *Inh*^r isolates with KatG(S315T), retaining catalase-peroxidase activities, may have a survival advantage, and this may explain the global spread of strains with the KatG(S315T) mutation.

ACKNOWLEDGMENTS

We thank Akiko Seshimo for excellent technical assistance.

This work was supported by Health Sciences Research grants (H21-SHINKO-IPPAN-016) and a Grant for International Health Research (21A-105) from the Ministry of Health, Labor and Welfare of Japan.

REFERENCES

- Ando, H., S. Mitarai, Y. Kondo, T. Suetake, J. I. Sekiguchi, S. Kato, T. Mori, and T. Kirikae. 2009. Pyrazinamide resistance in multidrug-resistant *Mycobacterium tuberculosis* isolates in Japan. Clin. Microbiol. Infect. [Epub ahead of print.] doi:10.1111/j.1469-0691.2009.03078.x.
- Aristimuno, L., R. Armengol, A. Cebollada, M. Espana, A. Guilarte, C. Lafoz, M. A. Lezcano, M. J. Revillo, C. Martin, C. Ramirez, N. Rastogi, J. Rojas, A. V. de Salas, C. Sola, and S. Samper. 2006. Molecular characterization of *Mycobacterium tuberculosis* isolates in the First National Survey of Anti-tuberculosis Drug Resistance from Venezuela. BMC Microbiol. 6:90.
- Aziz, M., A. Laszlo, M. Raviglione, H. Rieder, M. Espinal, and A. Wright. 2003. Guidelines for surveillance of drug resistance in tuberculosis, Second edition ed. World Health Organization, Geneva, Switzerland.

4. Bernstein, J., W. A. Lott, B. A. Steinberg, and H. L. Yale. 1952. Chemotherapy of experimental tuberculosis. V. Isonicotinic acid hydrazide (nydrazid) and related compounds. *Am. Rev. Tuberc.* **65**:357–364.
5. Bertrand, T., N. A. Eady, J. N. Jones, Jesmin, J. M. Nagy, B. Jamart-Gregoire, E. L. Raven, and K. A. Brown. 2004. Crystal structure of *Mycobacterium tuberculosis* catalase-peroxidase. *J. Biol. Chem.* **279**:38991–38999.
6. Brossier, F., N. Veziris, C. Truffot-Pernot, V. Jarlier, and W. Sougakoff. 2006. Performance of the genotype MTBDR line probe assay for detection of resistance to rifampin and isoniazid in strains of *Mycobacterium tuberculosis* with low- and high-level resistance. *J. Clin. Microbiol.* **44**:3659–3664.
7. Cardoso, R. F., R. C. Cooksey, G. P. Morlock, P. Barco, L. Cecon, F. Forestiero, C. Q. Leite, D. N. Sato, M. de Lourdes Shikama, E. M. Mami-zuka, R. D. Hirata, and M. H. Hirata. 2004. Screening and characterization of mutations in isoniazid-resistant *Mycobacterium tuberculosis* isolates obtained in Brazil. *Antimicrob. Agents Chemother.* **48**:3373–3381.
8. Dobner, P., S. Rusch-Gerdes, G. Bretzel, K. Feldmann, M. Rifai, T. Loscher, and H. Rinder. 1997. Usefulness of *Mycobacterium tuberculosis* genomic mutations in the genes *katG* and *inhA* for the prediction of isoniazid resistance. *Int. J. Tuberc. Lung Dis.* **1**:365–369.
9. Escalante, P., S. Ramaswamy, H. Sanabria, H. Soini, X. Pan, O. Valiente-Castillo, and J. M. Musser. 1998. Genotypic characterization of drug-resistant *Mycobacterium tuberculosis* isolates from Peru. *Tuber. Lung Dis.* **79**:111–118.
10. Espinal, M. A., A. Laszlo, L. Simonsen, F. Boulahbal, S. J. Kim, A. Reniero, S. Hoffner, H. L. Rieder, N. Binkin, C. Dye, R. Williams, and M. C. Raviglione. 2001. Global trends in resistance to antituberculosis drugs. World Health Organization-International Union against Tuberculosis and Lung Disease Working Group on Anti-Tuberculosis Drug Resistance Surveillance. *N. Engl. J. Med.* **344**:1294–1303.
11. Fang, Z., C. Doig, A. Rayner, D. T. Kenna, B. Watt, and K. J. Forbes. 1999. Molecular evidence for heterogeneity of the multiple-drug-resistant *Mycobacterium tuberculosis* population in Scotland (1990 to 1997). *J. Clin. Microbiol.* **37**:998–1003.
12. Fujiki, A. 2001. TB bacteriology examination to stop TB. The Research Institute of Tuberculosis, Tokyo, Japan.
13. Gagneux, S., M. V. Burgos, K. DeRiemer, A. Encisco, S. Munoz, P. C. Hopewell, P. M. Small, and A. S. Pym. 2006. Impact of bacterial genetics on the transmission of isoniazid-resistant *Mycobacterium tuberculosis*. *PLoS Pathog.* **2**:e61.
14. Haas, W. H., K. Schilke, J. Brand, B. Amthor, K. Weyer, P. B. Fourie, G. Bretzel, V. Sticht-Groh, and H. J. Bremer. 1997. Molecular analysis of *katG* gene mutations in strains of *Mycobacterium tuberculosis* complex from Africa. *Antimicrob. Agents Chemother.* **41**:1601–1603.
15. Homolka, S., E. Post, B. Oberhauser, A. G. George, L. Westman, F. Dafaie, S. Rusch-Gerdes, and S. Niemann. 2008. High genetic diversity among *Mycobacterium tuberculosis* complex strains from Sierra Leone. *BMC Microbiol.* **8**:103.
16. Lee, A. S., I. H. Lim, L. L. Tang, A. Telenti, and S. Y. Wong. 1999. Contribution of *kasA* analysis to detection of isoniazid-resistant *Mycobacterium tuberculosis* in Singapore. *Antimicrob. Agents Chemother.* **43**:2087–2089.
17. Loewen, P. C., J. Switala, M. Smolenski, and B. L. Triggs-Raine. 1990. Molecular characterization of three mutations in *katG* affecting the activity of hydroperoxidase I of *Escherichia coli*. *Biochem. Cell Biol.* **68**:1037–1044.
18. Marttila, H. J., H. Soini, E. Eerola, E. Vyshnevskaya, B. I. Vyshnevskiy, T. F. Otten, A. V. Vasilyef, and M. K. Viljanen. 1998. A Ser315Thr substitution in KatG is predominant in genetically heterogeneous multidrug-resistant *Mycobacterium tuberculosis* isolates originating from the St. Petersburg area in Russia. *Antimicrob. Agents Chemother.* **42**:2443–2445.
19. Marttila, H. J., H. Soini, P. Huovinen, and M. K. Viljanen. 1996. *katG* mutations in isoniazid-resistant *Mycobacterium tuberculosis* isolates recovered from Finnish patients. *Antimicrob. Agents Chemother.* **40**:2187–2189.
20. Mokrousov, I., O. Narvskaya, T. Otten, E. Limeschenko, L. Steklova, and B. Vyshnevskiy. 2002. High prevalence of KatG Ser315Thr substitution among isoniazid-resistant *Mycobacterium tuberculosis* clinical isolates from north-western Russia, 1996 to 2001. *Antimicrob. Agents Chemother.* **46**:1417–1424.
21. Nagy, J. M., A. E. Cass, and K. A. Brown. 1997. Purification and characterization of recombinant catalase-peroxidase, which confers isoniazid sensitivity in *Mycobacterium tuberculosis*. *J. Biol. Chem.* **272**:31265–31271.
22. Otsuka, Y., P. Parniewski, Z. Zwolska, M. Kai, T. Fujino, F. Kirikae, E. Toyota, K. Kudo, T. Kuratsuji, and T. Kirikae. 2004. Characterization of a trinucleotide repeat sequence (CGG)₅ and potential use in restriction fragment length polymorphism typing of *Mycobacterium tuberculosis*. *J. Clin. Microbiol.* **42**:3538–3548.
23. Piatek, A. S., A. Telenti, M. R. Murray, H. El-Hajj, W. R. Jacobs, Jr., F. R. Kramer, and D. Alland. 2000. Genotypic analysis of *Mycobacterium tuberculosis* from two distinct populations using molecular beacons: implications for rapid susceptibility testing. *Antimicrob. Agents Chemother.* **44**:103–110.
24. Pym, A. S., B. Saint-Joanis, and S. T. Cole. 2002. Effect of *katG* mutations on the virulence of *Mycobacterium tuberculosis* and the implication for transmission in humans. *Infect. Immun.* **70**:4955–4960.
25. Rossau, R., H. Traore, H. De Beenhouwer, W. Mijs, G. Jannes, P. De Rijk, and F. Portaels. 1997. Evaluation of the INNO-LiPA Rif. TB assay, a reverse hybridization assay for the simultaneous detection of *Mycobacterium tuberculosis* complex and its resistance to rifampin. *Antimicrob. Agents Chemother.* **41**:2093–2098.
26. Saint-Joanis, B., H. Suchon, M. Wilming, K. Johnsson, P. M. Alzari, and S. T. Cole. 1999. Use of site-directed mutagenesis to probe the structure, function and isoniazid activation of the catalase/peroxidase, KatG, from *Mycobacterium tuberculosis*. *Biochem. J.* **338**(3):753–760.
27. Sala, C., F. Forti, E. Di Florio, F. Canneva, A. Milano, G. Riccardi, and D. Ghisotti. 2003. *Mycobacterium tuberculosis* FurA autoregulates its own expression. *J. Bacteriol.* **185**:5357–5362.
28. Sekiguchi, J., T. Miyoshi-Akiyama, E. Augustynowicz-Kopec, Z. Zwolska, F. Kirikae, E. Toyota, I. Kobayashi, K. Morita, K. Kudo, S. Kato, T. Kuratsuji, T. Mori, and T. Kirikae. 2007. Detection of multidrug resistance in *Mycobacterium tuberculosis*. *J. Clin. Microbiol.* **45**:179–192.
29. Sekiguchi, J., T. Nakamura, T. Miyoshi-Akiyama, F. Kirikae, I. Kobayashi, E. Augustynowicz-Kopec, Z. Zwolska, K. Morita, T. Suetake, H. Yoshida, S. Kato, T. Mori, and T. Kirikae. 2007. Development and evaluation of a line probe assay for rapid identification of *pncA* mutations in pyrazinamide-resistant *Mycobacterium tuberculosis* strains. *J. Clin. Microbiol.* **45**:2802–2807.
30. van Doorn, H. R., P. E. de Haas, K. Kremer, C. M. Vandenbroucke-Grauls, M. W. Borgdorff, and D. van Soolingen. 2006. Public health impact of isoniazid-resistant *Mycobacterium tuberculosis* strains with a mutation at amino-acid position 315 of *katG*: a decade of experience in The Netherlands. *Clin. Microbiol. Infect.* **12**:769–775.
31. Victor, T. C., G. S. Pretorius, J. V. Felix, A. M. Jordaen, P. D. van Helden, and K. D. Eisenach. 1996. *katG* mutations in isoniazid-resistant strains of *Mycobacterium tuberculosis* are not infrequent. *Antimicrob. Agents Chemother.* **40**:1572.
32. Wei, C. J., B. Lei, J. M. Musser, and S. C. Tu. 2003. Isoniazid activation defects in recombinant *Mycobacterium tuberculosis* catalase-peroxidase (KatG) mutants evident in *InhA* inhibitor production. *Antimicrob. Agents Chemother.* **47**:670–675.
33. Wengenack, N. L., J. R. Uhl, A. L. St. Amand, A. J. Tomlinson, L. M. Benson, S. Naylor, B. C. Kline, F. R. Cockerill III, and F. Rusnak. 1997. Recombinant *Mycobacterium tuberculosis* KatG(S315T) is a competent catalase-peroxidase with reduced activity toward isoniazid. *J. Infect. Dis.* **176**:722–727.
34. Wilming, M., and K. Johnsson. 2001. Inter- and intramolecular domain interactions of the catalase-peroxidase KatG from *M. tuberculosis*. *FEBS Lett.* **509**:272–276.
35. Zhang, Y., B. Heym, B. Allen, D. Young, and S. Cole. 1992. The catalase-peroxidase gene and isoniazid resistance of *Mycobacterium tuberculosis*. *Nature* **358**:591–593.
36. Zhang, Y., and A. Telenti. 2000. Genetics of drug resistance in *Mycobacterium tuberculosis*. ASM Press, Washington, DC.